Cell Calcium 48 (2010) 1–9

Contents lists available at ScienceDirect

Cell Calcium

journal homepage: www.elsevier.com/locate/ceca

Activation of store-operated I_{CRAC} by hydrogen peroxide

Morten Grupe, George Myers, Reinhold Penner, Andrea Fleig*

Laboratory of Cell and Molecular Signaling, Center for Biomedical Research at The Queen's Medical Center and John A. Burns School of Medicine at the University of Hawaii, 1301 Punchbowl St., Honolulu, HI 96813, USA

ARTICLE INFO

Article history:
Received 4 February 2010
Received in revised form 14 May 2010
Accepted 18 May 2010
Available online 19 June 2010

Keywords:
Store-operated calcium entry
Orai
CRAC channel
H_2O_2
Reactive oxygen species
TRPM2 channel

ABSTRACT

Reactive oxygen species (ROS) such as hydrogen peroxide (H_2O_2) play a role in both innate immunity as well as cellular injury. H_2O_2 induces changes in intracellular calcium ($[Ca^{2+}]_i$) in many cell types and this seems to be at least partially mediated by transient receptor potential melastatin 2 (TRPM2) in cells that express this channel. Here we show that low concentrations of H_2O_2 induce the activation of the Ca^{2+}-release activated Ca^{2+} current I_{CRAC}. This effect is not mediated by direct CRAC channel activation, since H_2O_2 does not activate heterologously expressed CRAC channels independently of stromal interaction molecule (STIM). Instead, I_{CRAC} activation is partially mediated by store depletion through activation of inositol 1,4,5 trisphosphate receptors (IP_3R), since pharmacological inhibition of IP_3 receptors by heparin or molecular knock-out of all IP_3 receptors in DT40 B cells strongly reduce H_2O_2-induced I_{CRAC}. The remainder of H_2O_2-induced I_{CRAC} activation is likely mediated by IP_3R-independent store-depletion. Our data suggest that H_2O_2 can activate Ca^{2+} entry through TRPM2 as well as store-operated CRAC channels, thereby adding a new facet to ROS-induced Ca^{2+} signaling.

1. Introduction

Reactive oxygen species (ROS) are a group of molecules and ions with the potential of causing cellular damage due to their highly reactive characteristics. Hydrogen peroxide (H_2O_2), an oxidizing agent and member of ROS, is often used in experimental models of oxidative stress, although accumulating evidence indicates that H_2O_2 may also function as an important signaling molecule in diverse cellular processes such as cell development, proliferation, signal transduction and protein regulation [1]. Thus, ROS and intracellular Ca^{2+} have shown interdependent relations in numerous processes [2], thereby linking ROS to one of the most diverse second messengers in the cell. H_2O_2 is constantly produced in the cell as a by-product of aerobic metabolism in the mitochondria. To prevent toxic ROS overload, several enzymatic mechanisms will catalyze the conversion of H_2O_2 to water and oxygen, including peroxisomal catalase and cytosolic peroxiredoxins and glutathione peroxidase. For a long time, H_2O_2 was believed to freely cross membranes, but more recent evidence suggests that the membrane permeability is regulated by the composition of the membrane as well as diffusion facilitation through aquaporins [3].

The broad effects of H_2O_2 on enzymes, growth factors, transcription factors and ion channels are believed to mainly occur through redox modification of reactive thiol groups in cysteine residues [4]. Although various ion channels are modulated by ROS [4,5], the only known ion channel that can be gated through actions of H_2O_2 is the Ca^{2+} permeable non-selective cation channel TRPM2 (transient-receptor potential melastatin-2) [6–8]. The channel's primary agonist is adenosine diphosphoribose (ADPR) [9,10]. Intracellular Ca^{2+}, H_2O_2 or related nucleotides such as cyclic adenosine diphosphoribose (cADPR) and nicotinic acid adenine dinucleotide phosphate (NAADP) have limited if any direct gating activities [7,11], although they can synergize with ADPR to activate TRPM2 currents at lower ADPR concentrations [7,12]. For H_2O_2-mediated activation of TRPM2 both ADPR-dependent and -independent mechanisms have been suggested [8,13]. Additional channel targets of H_2O_2 include the ryanodine receptor (RyR), which functions as a Ca^{2+}-release channel in muscle cells and neurons [14] and an outwardly rectifying cation current, I_{OGD}, in murine cortical neurons, presumably involving TRPM7 channels [15]. Additionally, H_2O_2 at millimolar concentration can induce a sustained nonselective cation current, I_{LiNC}, independent of ion channels [16].

The major route of Ca^{2+} entry in nonexcitable cells is via store-operated channels (SOC). The best characterized SOC is the Ca^{2+} release-activated Ca^{2+} channel (CRAC), a highly selective low-conductance Ca^{2+} channel, which is activated by depletion of internal Ca^{2+} stores [17]. Molecularly, this involves stromal interaction molecule 1 (STIM1), which senses ER Ca^{2+} levels [18,19] and upon store depletion activates the plasma membrane channel CRACM1 (also called Orai1) [20–22]. Store-operated Ca^{2+} entry (SOCE) is a widely expressed mechanism in many cells that respond to ROS, however, little is known about effects of ROS on the store-

* Corresponding author. Tel.: +1 808 537 7931; fax: +1 808 537 7939.
E-mail address: afleig@hawaii.edu (A. Fleig).

0143-4160/$ – see front matter © 2010 Elsevier Ltd. All rights reserved.
doi:10.1016/j.ceca.2010.05.005

operated CRAC current (I_{CRAC}). We set out to assess possible effects of ROS on I_{CRAC} using calcium imaging and whole-cell electrophysiology. We report that extracellular application or intracellular perfusion of H_2O_2 at micromolar concentrations activates I_{CRAC} in several native cell lines independent of the presence or absence of TRPM2-like currents.

2. Methods

2.1. Cell culture

Cells were incubated at 37 °C with 5% CO_2 in the appropriate cell media. Tetracycline-inducible HEK293 TRPM2-expressing cells were cultured in DMEM with 10% fetal bovine serum (FBS) supplemented with blasticidin (5 μg/ml, Invitrogen) and zeocin (0.4 mg/ml, Invitrogen) [9], RBL-2H3 cells in DMEM with 10% FBS, Jurkat T-lymphocytes in RPMI 1640 with 10% FBS, HEK293 CRACM1-overexpressing cells in DMEM with 10% FBS [23], and DT40 B-lymphocytes in RPMI 1640 with 10% FBS supplemented with 5% chicken serum and 2 mM L-glutamine. For induction of TRPM2 expression, HEK293 cells were resuspended in medium containing 1 μg/ml tetracycline (Invitrogen) 4–8 h before experiments.

2.2. Solutions and chemicals

For fluorescence and patch-clamp measurements cells were kept in standard extracellular saline solution (in mM): 140 NaCl, 2.8 KCl, 2 $MgCl_2$, 11 glucose, 10 HEPES–NaOH. $CaCl_2$ concentration was 1 mM in calcium imaging experiments and 10 mM in patch-clamp experiments unless otherwise stated. Neutral pH was between 7.2 and 7.3, adjusted with NaOH and osmolarity was 300 mOsm. For the TRPM2 inhibition panel the divalent and trivalent cations (Ba^{2+}, Cd^{2+}, Co^{2+}, Cu^{2+}, Ni^{2+}, Sr^{2+}, Zn^{2+}, and La^{3+}) were added as chloride salts into the standard extracellular solution at 1 mM. In some experiments 1 μM $LaCl_3$ was included in the extracellular solution. H_2O_2 (30% stock solution) was added in various concentrations to extra- and intracellular solutions.

Standard pipette filling solutions contained (in mM): 140 Cs-glutamate, 8 NaCl, 1 $MgCl_2$, 10 HEPES–CsOH. In patch-clamp recordings with DT40 cells $MgCl_2$ concentration was increased to 3 mM to inhibit endogenous TRPM7 currents. Ca^{2+} concentration was buffered to 150 nM, 200 nM or 500 nM in whole-cell experiments, calculated with WebMaxC (http://www.stanford.edu/~cpatton/webmaxc/webmaxcS.htm), with 10 mM Cs-BAPTA and 4 mM, 4.55 mM or 6.9 mM $CaCl_2$, respectively, or left unbuffered. ADPR was added to the pipette solution in TRPM2 experiments. In some experiments heparin was added to the pipette solution. IP_3 and thapsigargin (dissolved in DMSO) was used in some experiments to activate I_{CRAC}. All chemicals were purchased from Sigma–Aldrich (St. Louis, MO, USA), except H_2O_2 (Fisher Scientific, Hampton, NH, USA).

2.3. Electrophysiology

Patch-clamp experiments were performed in whole-cell configuration at 21–25 °C. Patch pipettes were pulled from glass capillaries (Kimble Products, Fisher Scientific, USA) on a DMZ-Universal Puller (DAGAN, Minneapolis, MN) with pipette resistances in the range of 2–3 MΩ. Data were acquired with Patchmaster software controlling an EPC-10 amplifier (HEKA, Lambrecht, Germany). Voltage ramps of 50 ms spanning the voltage range of −100 mV to 100 mV were applied from a holding potential of 0 mV at a rate of 0.5 Hz, unless otherwise stated. Experiments were recorded typically over periods of 100–600 s. Voltages were corrected for liquid junction potentials of 10 mV. Capacitive currents and series resistances were determined and corrected before each voltage ramp. The low-resolution temporal development of currents for a given potential was extracted from the leak-corrected individual ramp currents by measuring current amplitudes at voltages of −80 mV and +80 mV, unless otherwise stated.

2.4. Single channel measurements

TRPM2 single channel recordings in Jurkat T cells were performed in the whole-cell configuration. A ramp from −100 mV to +10 mV over 11 s was applied continuously. Currents were filtered at 50 Hz. Linear fits were performed from −100 mV to 0 mV in Igor Pro (Wavemetrics, Oregon, USA) to determine the single channel conductance b according to a line function $a + bx$.

2.5. Fluorescence measurements

For measurement of cytosolic Ca^{2+} concentration cells were loaded with 5 μM Fura-2 AM (acetoxymethylester, Molecular Probes) for 30 min in 37 °C, washed and kept in external solution. Experiments were performed with an Olympus BX2 fluorescence microscope equipped with a dual excitation fluorometric imaging system (TILL-Photonics). Data acquisition and computation was controlled by TILLvisION software. Dye-loaded cells were excited by wavelengths of 340 nm and 380 nm for 20 ms each, produced by a monochromator (Polychrome IV). The fluorescence emission of several single cell bodies was simultaneously recorded with a video camera (TILL-Photonics Imago) with an optical 440 nm longpass filter. The signals were sampled at 0.5 Hz and computed into relative ratio units of the fluorescence intensity at the different wavelengths (340/380 nm).

2.6. Subcloning and overexpression

Full length human STIM1 was subcloned as described earlier [24]. For electrophysiological analysis, STIM1 proteins were overexpressed in HEK293 cells stably expressing CRACM1 [25] using lipofectamine 2000 (Invitrogen) and the GFP expressing cells were selected by fluorescence. Experiments were performed 24–48 h post-transfection.

2.7. Data analysis

Data was analyzed with FitMaster (HEKA, Lambrecht, Germany) and Igor Pro (WaveMetrics, Oregon, USA). Where applicable, statistical errors of averaged data are given as means ± SEM with n determinations. Single ramps were plotted as current–voltage relationships. Currents were normalized to cell size in pF, unless otherwise stated. Half-maximal activation time was calculated with a minimum–maximum dose–response function, $f(t) = Y_{min} + (Y_{max} - Y_{min}) \times (1/(1 + (K_d/t)^n)$, where Y_{min} is current basal level, Y_{max} is the current plateau phase, K_d is half-maximal activation time and n is an integer. Statistical calculations were performed using Igor Pro. Significance levels were determined by Student's t-test. $P < 0.05$ was considered to be significant.

3. Results

3.1. TRPM2 currents are not significantly affected by divalent or trivalent ions

H_2O_2 is a well-known activator of TRPM2 currents [6–8]. We pursued two strategies to differentiate H_2O_2-induced Ca^{2+} influx through TRPM2 from other Ca^{2+} entry pathways, including I_{CRAC}. The first strategy involved the use of cell lines that differentially

express I_{CRAC} and TRPM2 and the second was based on differential pharmacological inhibition. Known blockers of TRPM2, such as 2-amino-ethoxydiphenyl borate (2-APB), flufenamic acid or clotrimazole [26,27] also interfere with store-operated calcium entry [28–30]. Lanthanum (La^{3+}), however, potently blocks I_{CRAC} [31], but reportedly does not inhibit TPRM2 activity [32]. We tested various divalent cations and La^{3+} for inhibitory actions on TRPM2 currents in whole-cell patch-clamp experiments in HEK293 cells stably expressing TRPM2 under a tetracycline-inducible promoter. Cells were kept in a standard NaCl-based extracellular solution with 1 mM $CaCl_2$ and perfused with a standard Cs-glutamate-based intracellular solution supplemented with 500 μM ADPR (see Section 2). Within seconds of whole-cell break-in, large currents developed (Fig. 1A) with the typical linear current–voltage (I/V) relationship of TRPM2 (Fig. 1B), reaching several *nA* at −80 mV. In order to measure the inhibition of TRPM2, currents were allowed to reach the plateau phase before application of 1 mM of various divalent cations or La^{3+} at 60 s. When applying Ba^{2+}, Cu^{2+}, Ni^{2+}, Cd^{2+}, Sr^{2+}, or Co^{2+} current reduction was less than 5% and Zn^{2+} and La^{3+} reduced currents by just 5–7% (Fig. 1C). In each case, the current reduction was reversible as seen by the increase in current following removal of the cations at 120 s. This demonstrates that TRPM2 is not markedly affected by divalent ions or La^{3+}, in marked contrast to many other ion channels, including I_{CRAC} [31].

3.2. H_2O_2 causes Ca^{2+} release and Ca^{2+} influx independent of TRPM2

Using Fura-2 calcium imaging, we assessed Ca^{2+}-permeable ion channels as candidates for H_2O_2-mediated Ca^{2+} signals in various cell types that express I_{CRAC} with or without TRPM2. Jurkat T lymphocytes express both I_{CRAC} and TRPM2 natively [11,33], whereas RBL-2H3 (Fig. S1A; [34]) and wild-type (WT) HEK293 express only I_{CRAC} [9,21]. In the latter cell type, we additionally overexpressed TRPM2 heterologously. Cells were bathed in standard external NaCl-based bath solution with 1 mM Ca^{2+} and then exposed for 3 min to 100 μM H_2O_2 in Ca^{2+}-free bath solution to reveal internal Ca^{2+} release, followed by readmission of 1 mM Ca^{2+} to reveal possible Ca^{2+} entry. In RBL-2H3 cells, H_2O_2 induced both Ca^{2+} release and a relatively small Ca^{2+}influx component when returning to 1 mM Ca^{2+} (Fig. 2A). Since RBL-2H3 cells do not produce ADPR-induced TRPM2 currents (Fig. S1A) and H_2O_2 caused large Ca^{2+} release, we assessed Ca^{2+} entry through I_{CRAC} by performing identical experiments in the presence of 1 μM La^{3+}, a highly potent blocker of I_{CRAC} [31]. This revealed that a portion of the Ca^{2+} signal observed after readmission of Ca^{2+} was mediated by La^{3+}-sensitive Ca^{2+} influx (Fig. 2A).

This was confirmed in HEK293 WT cells, where H_2O_2-induced Ca^{2+} release was followed by a Ca^{2+} signal upon Ca^{2+} readmission that could also be inhibited by 1 μM $LaCl_3$ (Fig. 2B). It should be noted that in HEK293 WT cells 20 μM H_2O_2 was sufficient to evoke reliable Ca^{2+} responses, whereas in RBL-2H3 cells the H_2O_2 concentration had to be increased to 100 μM to reliably induce Ca^{2+} entry upon Ca^{2+} readmission. We next investigated Ca^{2+} release and Ca^{2+} influx in tetracycline-induced HEK293–TRPM2 cells. Applying 20 μM H_2O_2 resulted in Ca^{2+} release and substantial Ca^{2+} influx both in the absence and presence of 1 μM $LaCl_3$ (Fig. 2C). This confirms that H_2O_2 can activate TRPM2 and that La^{3+} fails to block TRPM2.

We also investigated Jurkat T cells, which express TRPM2 and CRAC channels natively. Here, application of 20 μM H_2O_2 revealed Ca^{2+} release as well as Ca^{2+} influx when returning to 1 mM Ca^{2+} (Fig. 2D). To assess whether the Ca^{2+} entry upon readmission of Ca^{2+} involved TRPM2 activity, we performed the same experiment in the presence of 1 μM $LaCl_3$, which has negligible inhibitory effects on TRPM2 (as seen in Figs. 1 and 2C). Again H_2O_2 induced a Ca^{2+} release, but Ca^{2+} entry was completely blocked (Fig. 2D), demonstrating that in Jurkat T cells the H_2O_2-mediated Ca^{2+} influx caused by 20 μM H_2O_2 was not related to TRPM2.

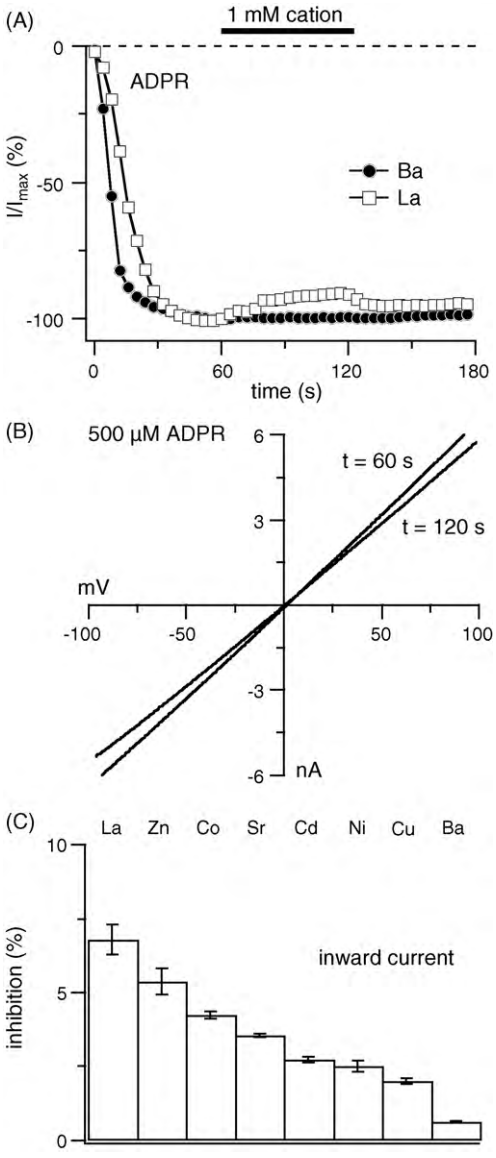

Fig. 1. Inhibition of TRPM2 current by various divalent and trivalent cations. (A) Average TRPM2 currents in tetracycline-induced HEK293 cells (1 μg/ml, 4–8 h) perfused with Cs-glutamate based pipette solution containing 500 μM ADPR with unbuffered internal Ca^{2+}. Currents were normalized to the data point prior to cation application. The bar indicates application of 1 mM of each cation ($n = 5$ for each condition), displayed is the Ba^{2+} and La^{3+} trace. Currents were measured with a voltage ramp from −100 to +100 mV over 50 ms at 0.5 Hz intervals from a holding potential of 0 mV. Inward currents were extracted at −80 mV, averaged and plotted versus time. (B) Representative current–voltage (I/V) relationship of ADPR-activated TRPM2 current in HEK293 cells at $t = 60$ s and upon application of 1 mM La^{3+} at $t = 120$ s. (C) Degree of inhibition of TRPM2 by 1 mM of various di- and trivalent ions. Values represent mean (±SEM) over the 60 s period of application.

For all cell types investigated, the H_2O_2-induced Ca^{2+} signals trended back to the baseline in control experiments without Ca^{2+} readmission, but did not return entirely. The incomplete return to baseline may be due to an additional effect of H_2O_2 on the plasma membrane Ca^{2+} ATPase (PMCA). It has been previously reported that La^{3+} can cause an apparent prolongation of the release response due to a block of PMCA [35]. However, our data would imply that H_2O_2 is less potent than 1 μM La^{3+} in blocking PMCA. Our control data also provides evidence that Ca^{2+} entry through

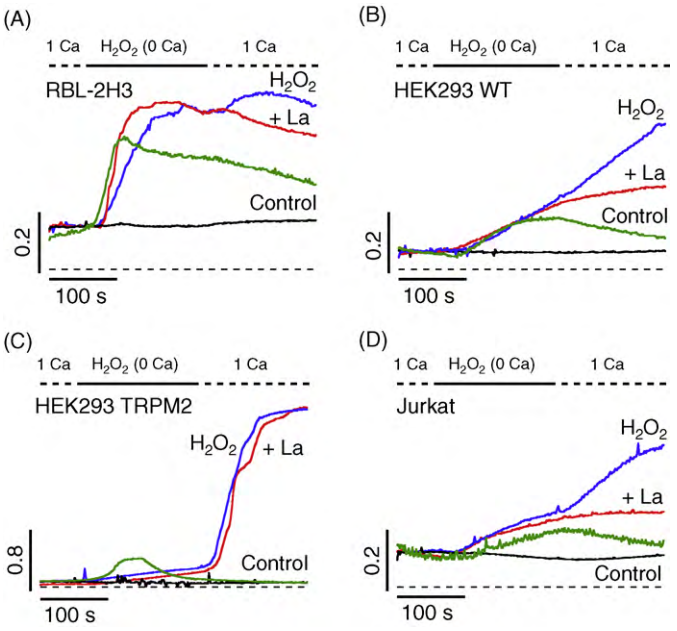

Fig. 2. H_2O_2 induces Ca^{2+} response in RBL-2H3 cells, HEK293 cells and Jurkat T cells. (A) Averaged changes in $[Ca^{2+}]_i$ measured as ratios of Fura-2 fluorescence excited at 340 and 380 nm in Fura-2 AM loaded RBL-2H3 cells in response to H_2O_2. Cells were kept in a saline solution with 1 mM $CaCl_2$ in the absence (blue trace, $n = 34$) or presence of 1 μM $LaCl_3$ (red trace, $n = 35$). Black bar indicates application of 100 μM H_2O_2 in nominally Ca^{2+} free saline solution. In controls H_2O_2 was omitted from the Ca^{2+} free saline solution (black trace, $n = 57$) and $CaCl_2$ was omitted from the readmission solution (green trace, $n = 42$). Cells were loaded with 5 uM Fura-2 AM at 37 °C for 30 min. Traces are representative of three independent experiments performed on different days. (B) Experimental protocol as in (A) but for Fura-2 AM loaded HEK293 WT cells in the absence (blue trace, $n = 24$) or presence of 1 μM $LaCl_3$ (red trace, $n = 6$). Black bar indicates application of 20 μM H_2O_2 in Ca^{2+} free saline solution. In controls H_2O_2 was omitted from the Ca^{2+} free saline solution (black trace, $n = 28$) and $CaCl_2$ was omitted from the readmission solution (green trace, $n = 52$). Traces are representative of three independent experiments performed on different days. (C) Experimental protocol as in (A) but for Fura-2 AM loaded tetracycline-induced (1 μg/ml, 21–22 h) HEK293 cells expressing TRPM2 in the absence (blue trace, $n = 16$) or presence of 1 μM $LaCl_3$ (red trace, $n = 13$). Black bar indicates application of 20 μM H_2O_2 in Ca^{2+} free saline solution. In controls H_2O_2 was omitted from the Ca^{2+} free saline solution (black trace, $n = 9$) and $CaCl_2$ was omitted from the readmission solution (green trace, $n = 28$). (D) Experimental protocol as in (A) but for Fura-2 AM loaded Jurkat T cells in the absence (blue trace, $n = 74$) or presence of 1 μM $LaCl_3$ (red trace, $n = 126$). Black bar indicates application of 20 μM H_2O_2 in nominally Ca^{2+} free saline solution. In controls H_2O_2 was omitted from the Ca^{2+} free saline solution (black trace, $n = 49$) and $CaCl_2$ was omitted from the readmission solution (green trace, $n = 15$). Traces are representative of three independent experiments performed on different days. (For interpretation of the references to colour in this figure legend, the reader is referred to the web version of the article.)

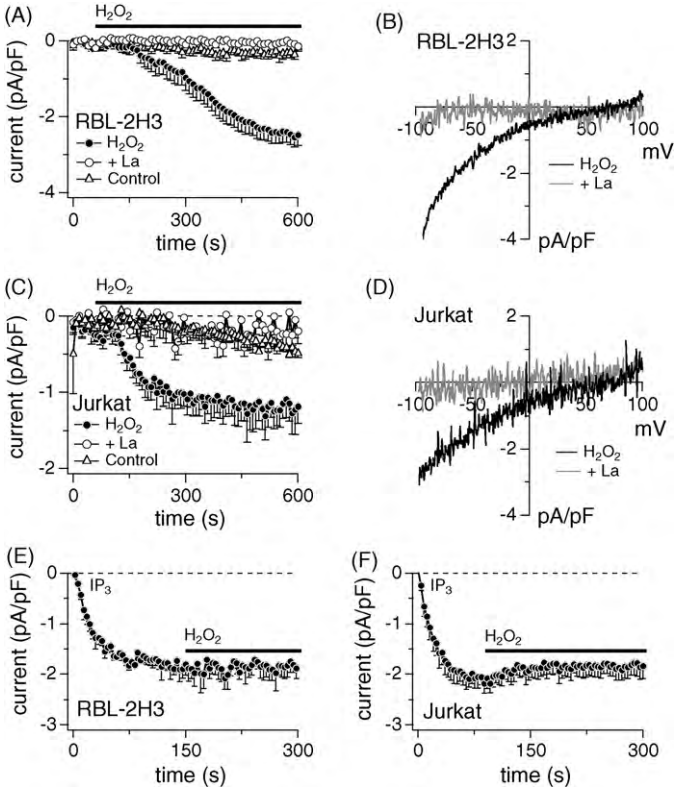

Fig. 3. H_2O_2 activates I_{CRAC} in RBL-2H3 cells and Jurkat T cells. (A) Average current development in RBL-2H3 cells induced by extracellular application of H_2O_2 in the absence (filled circles, $n = 12$) or presence of 1 μM $LaCl_3$ in the bath solution (open circles, $n = 5$). In control experiments H_2O_2 was omitted (open triangles, $n = 9$). Experiments were performed using Cs-glutamate based pipette solution with $[Ca^{2+}]_i$ clamped to 150 nM free Ca^{2+} with 10 mM Cs-BAPTA. The bar indicates application of 40 μM H_2O_2. Currents were measured with a voltage ramp from −100 to +100 mV over 50 ms at 0.5 Hz intervals from a holding potential of 0 mV. Inward currents were extracted at −80 mV and plotted versus time. Error bars indicate SEM. (B) Representative *I*/*V* relationship of H_2O_2-activated CRAC current in RBL-2H3 cells at $t = 600$ s in the absence (black trace) or presence of 1 μM $LaCl_3$ (grey trace). (C) Average current development in Jurkat T cells by extracellular application of H_2O_2 in the absence (filled circles, $n = 5$) or presence of 1 μM $LaCl_3$ in the bath solution (open circles, $n = 9$). In control experiments H_2O_2 was omitted (open triangles, $n = 5$). $[Ca^{2+}]_i$ was clamped to 200 nM free Ca^{2+} with 10 mM Cs-BAPTA and $[Mg^{2+}]_i$ was 3 mM. The bar indicates application of 80 μM H_2O_2. Currents were analyzed as in (A). (D) Representative *I*/*V* relationship of H_2O_2-activated CRAC current in Jurkat T cells at $t = 600$ s in the absence (black trace) or presence of 1 μM $LaCl_3$ (grey trace). (E) Average current density of I_{CRAC} extracted at −80 mV in RBL-2H3 cells perfused with 20 μM IP_3 ($n = 5$). The bar indicates application of 40 μM H_2O_2. (F) Average current density of I_{CRAC} extracted at −80 mV in Jurkat T cells perfused with 20 μM IP_3 ($n = 5$). The bar indicates application of 40 μM H_2O_2.

I_{CRAC} is more significant than the difference between the H_2O_2 and $H_2O_2 + La^{3+}$ traces suggests. Together, these findings indicate that extracellular application of H_2O_2 at low micromolar concentrations can activate a Ca^{2+} influx pathway in Jurkat T cells, HEK293 WT cells and RBL-2H3 cells that is not related to TRPM2 activity.

3.3. H_2O_2 induces I_{CRAC} in RBL-2H3 and Jurkat T cells

To determine whether the H_2O_2-activated Ca^{2+} influx observed in Ca^{2+} imaging experiments was mediated by I_{CRAC}, we performed whole-cell patch-clamp experiments. We used standard experimental conditions optimized for measuring I_{CRAC}, i.e. NaCl-based extracellular solution with 10 mM $CaCl_2$ and Cs-glutamate-based intracellular solution buffered to 150 nM free Ca^{2+} with Cs-BAPTA (see Section 2). In whole-cell patch-clamp experiments with RBL-2H3 cells, 10 mM CsCl was included in the bath solution to inhibit the inward-rectifier potassium current. We first tested for I_{CRAC} activation in RBL-2H3 cells by extracellular application of 40 μM H_2O_2 from a wide-tipped puffer pipette 1 min after break-in. As shown in Fig. 3A, H_2O_2 application activated an inward current in 12 out of 14 cells, reaching a plateau of -2.5 ± 0.3 pA/pF at 600 s with a half-maximal activation time of 281 ± 1.2 s. No current developed in two cells. The current exhibited inward rectification that is typical for I_{CRAC} [17] as illustrated in a representative *I*/*V* relationship (Fig. 3B). When including 1 μM $LaCl_3$ in the bath and application solution no inward current developed (Fig. 3A). In control experiments without H_2O_2 application, no significant inward currents developed (Fig. 3A).

Similar experiments were performed using Jurkat T cells. To effectively suppress spontaneous activation of I_{CRAC} in these cells, $[Ca^{2+}]_i$ was buffered to 200 nM and $[Mg^{2+}]_i$ was increased to 3 mM to suppress activation of endogenous TRPM7 currents. Application of 40 μM H_2O_2 did not activate inward currents consistently, however, 80 μM H_2O_2 activated an inward current in 5 of 5 cells. Currents reached a plateau of ~−1.2 pA/pF at 600 s with a half-

maximal activation time of 115 ± 3.3 s (Fig. 3C) and exhibited the typical inwardly rectifying *I*/*V* relationship for I_{CRAC} (Fig. 3D). The H_2O_2-induced current could be completely blocked by 1 μM $LaCl_3$ in the bath solution (Fig. 3C). No significant inward current developed in control experiments when cells were not exposed to H_2O_2 (Fig. 3C). In summary, these data provide evidence for the ability of H_2O_2 to activate I_{CRAC} in Jurkat T cells and in RBL-2H3 cells. It should be noted that none of the cells showed any sign of seal breakdown or increased leak current due to application of H_2O_2 at the concentrations used and neither did we observe development of any significant non-specific currents.

ROS are known to have a potential damaging effect on molecules such as DNA, proteins and lipids. We therefore investigated if H_2O_2, in addition to its activating qualities, exerted a negative effect on I_{CRAC}. We activated I_{CRAC} by perfusing cells with 20 μM IP_3 and internal Ca^{2+} buffered to 150 nM and then applied H_2O_2 after I_{CRAC} had fully developed. In RBL-2H3 cells, we did not see any inhibiting effect of 40 μM H_2O_2 on I_{CRAC} (Fig. 3E) and in Jurkat T cells, CRAC currents were slightly reduced by about ~15% during application of 40 μM H_2O_2 (Fig. 3F). The relative lack of effect of H_2O_2 after I_{CRAC} activation by IP_3 is further evidence that the current activated by H_2O_2 is exclusively I_{CRAC} and not caused by other non-specific or previously unknown currents.

3.4. H_2O_2-induced I_{CRAC} activation is partially mediated by IP_3 receptors

Next, we sought to determine the underlying mechanism of I_{CRAC} activation by H_2O_2. First, we addressed whether H_2O_2 activates I_{CRAC} due to store-independent and direct interaction with the pore-forming unit CRACM1.

This was investigated in HEK293 cells stably overexpressing CRACM1 with only endogenous STIM molecules present [23]. These cells produce small IP_3-induced I_{CRAC} that is limited in size by the endogenous STIM molecules, as both CRACM and STIM proteins are needed to form CRAC channels that are regulated by store-depletion [24]. Whole-cell patch-clamp experiments were performed under conditions similar to those used in RBL-2H3 (Fig. 3). Application of 40 μM H_2O_2 produced a large inward current of −26.7 ± 10.6 pA/pF at 300 s in STIM1-transfected CRACM1-overexpressing HEK-293 cells and no significant current response in non-transfected cells (Fig. 4A). Representative *I*/*V* relationships for these cells are shown in Fig. 4B. This indicates that H_2O_2 does not activate CRAC channels directly, but rather through store depletion and STIM1-dependent gating.

H_2O_2 can induce Ca^{2+} release in a variety of cells and one proposed mechanism is through activation of IP_3 receptors (IP_3R) [36,37], leading to activation of I_{CRAC} [17] (see Fig. 3A). To determine if the IP_3 pathway is involved in the activation of I_{CRAC} by H_2O_2, we perfused RBL-2H3 cells with 100 μg/ml heparin, an antagonist of IP_3 receptors [38]. When applying 40 μM H_2O_2, heparin slowed the activation kinetics of I_{CRAC} and reduced its amplitude as illustrated in Fig. 4C. In the presence of heparin, I_{CRAC} developed with a half-maximal activation time of 313 ± 1.8 s compared to 281 ± 1.2 s in its absence, and reaching an amplitude of −1.6 ± 0.2 pA/pF at 600 s compared to −2.5 ± 0.3 pA/pF in controls without heparin. A representative *I*/*V* relationship of CRAC currents in the presence of heparin is shown in Fig. 4D. These results further indicate that IP_3R activity may be partly responsible for mediating the H_2O_2-activated I_{CRAC}, although at present we cannot distinguish between direct IP_3R effects and/or possible effects on IP_3 mobilization.

3.5. H_2O_2-induced activation of I_{CRAC} independent of IP_3R

To further investigate the role of IP_3 receptors in H_2O_2-activated I_{CRAC}, we conducted patch-clamp experiments in a wild-type chicken DT40 B-lymphocyte cell line (DT40 WT) expressing all three IP_3 receptor isoforms (types I, II and III) as well as a genetically modified DT40 cell line in which all three IP_3 receptor isoforms are knocked out (DT40 KO) [39]. As DT40 cells develop very small I_{CRAC}, we optimized experimental conditions by increasing the external $CaCl_2$ concentration to 20 mM and expanding the voltage ramp to −150 mV, extracting current amplitudes at −130 mV [40]. Furthermore internal $MgCl_2$ concentration was increased to 3 mM to inhibit endogenous TRPM7 currents. In DT40 cells, TRPM2 does not contribute to the H_2O_2 effects, since perfusing these cells with 1 mM ADPR failed to induce any currents (Fig. S1B).

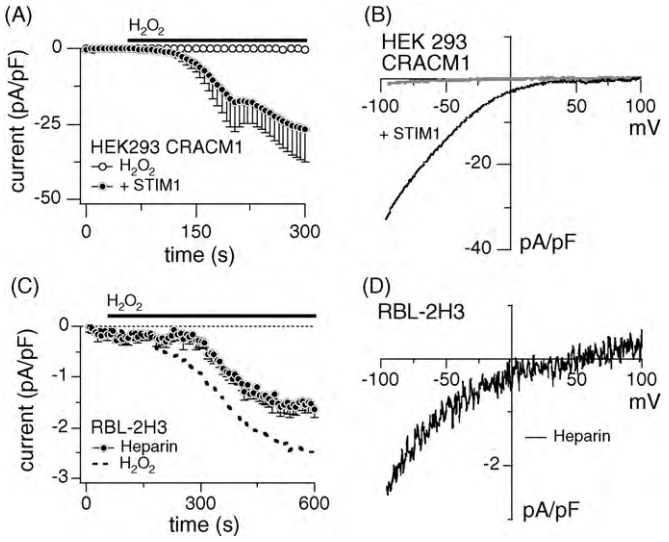

Fig. 4. Involvement of IP_3 receptors in H_2O_2-activated I_{CRAC}. (A) Average current density extracted at −80 mV in HEK293 cells stably overexpressing CRACM1 with (filled circles, $n = 4$) and without (open circles, $n = 5$) transfection of STIM1. The bar indicates application of 40 μM H_2O_2. Experiments were performed using Cs-glutamate based pipette solution with $[Ca^{2+}]_i$ clamped to 150 nM free Ca^{2+} with 10 mM Cs-BAPTA. Currents were measured with a voltage ramp from −100 to +100 mV over 50 ms at 0.5 Hz intervals from a holding potential of 0 mV. Error bars indicate SEM. (B) Representative *I*/*V* relationship in response to application of 40 μM H_2O_2 at 300 s in HEK293 cells overexpressing CRACM1 with (black trace) and without transfection of STIM1 (grey trace). (C) Average current density extracted at −80 mV in RBL-2H3 cells activated by extracellular application of 40 μM H_2O_2 with perfusion of 100 μg/ml heparin (filled circles, $n = 5$). The bar indicates application of 40 μM H_2O_2. For comparison the H_2O_2-activated I_{CRAC} trace (Fig. 3A) is included in the figure (dashed line). (D) Representative *I*/*V* relationship of H_2O_2-activated CRAC current in RBL-2H3 cells at −600 s when perfused with 100 μg/ml heparin (mean of 4 ramps).

We tested the two cell lines for IP_3-activated I_{CRAC} by perfusing cells with 20 μM IP_3. In WT cells, I_{CRAC} developed immediately in 4 out of 4 cells reaching a plateau of −1.2 ± 0.2 pA/pF at ~75 s, whereas KO cells did not show any current development (Fig. 5A). Neither WT nor KO cells developed I_{CRAC} in the absence of IP_3 with Ca^{2+} buffered to 150 nM (Fig. 5B). However, the DT40 KO cells have previously been shown to activate endogenous I_{CRAC} when stores are depleted independent of IP_3 receptors [40]. To confirm these previous observations we applied 10 μM thapsigargin (Tg) at 60 s resulting in I_{CRAC} development (Fig. 5C). Representative I/V relationships for the IP_3 and Tg experiments are displayed in Fig. 5D. Next, we assessed whether H_2O_2 could activate I_{CRAC} in DT40 cells by applying 40 and 100 μM H_2O_2 from a wide-tipped puffer pipette at 60 s, but as this resulted in no clear I_{CRAC} (data not shown), we included 40 μM H_2O_2 in the pipette solution. In WT cells this resulted in a slowly developing I_{CRAC}-like current in 4 out of 4 cells reaching an amplitude of ~−1.2 pA/pF at 300 s (Fig. 5E). In DT40 KO cells an inward current with smaller amplitude of ~−0.5 pA/pF at 300 s could be observed (Fig. 5E). This is significantly smaller than the amplitude in DT40 WT cells ($P < 0.05$). The averaged cur-

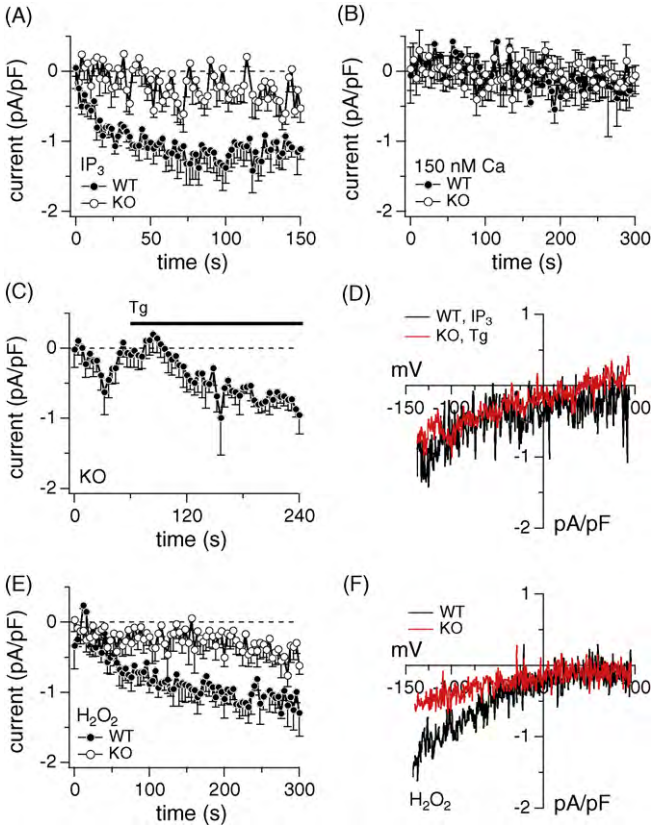

Fig. 5. Activation of I_{CRAC} in wild-type and complete IP_3 receptor-knockout DT40 B cells. (A) Average current density in DT40 wild-type (WT) (filled circles, $n = 4$) and complete (types I, II, III) knock-out (KO) cells (open circles, $n = 4$) when perfused with 20 μM IP_3. Extracellular $CaCl_2$ concentration was 20 mM and intracellular $MgCl_2$ concentration was 3 mM. Currents were measured with a voltage ramp from −150 to +100 mV over 50 ms at 0.5 Hz intervals from a holding potential of 0 mV. Inward currents were extracted at −130 mV, averaged and plotted versus time. (B) Average current density extracted at −130 mV in DT40 WT (filled circles, $n = 7$) and KO cells (open circles, $n = 8$) with internal Ca^{2+} buffered to 150 nM. (C) Average current density extracted at −130 mV in DT40 KO cells in response to application of 10 μM thapsigargin (Tg) as indicated by the bar ($n = 6$). (D) Representative *I*/*V* relationship of IP_3-perfused DT40 WT cells at $t = 150$ s and Tg-stimulated DT40 KO cells (red trace, mean of 6 ramps) at $t = 240$ s. (E) Average current density extracted at −130 mV in DT40 WT (filled circles, $n = 4$) and KO (open circles, $n = 10$) when internally perfused with 40 μM H_2O_2. (F) Representative *I*/*V* relationship of H_2O_2-perfused DT40 WT (black trace, mean of 4 ramps) and KO cells (red trace, mean of 10 ramps) at $t = 300$ s. (For interpretation of the references to colour in this figure legend, the reader is referred to the web version of the article.)

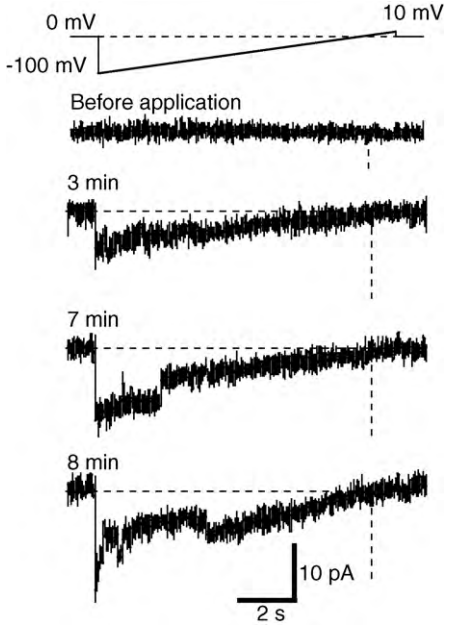

Fig. 6. Activation of TRPM2 channels by H_2O_2 in Jurkat T cells. Single channel activity of a representative cell measured with long voltage ramps in the whole-cell configuration. Two single channels activated when exposed to 100 μM H_2O_2 from 65 s (dotted lines indicate channel open levels). First single channel activity was observed at 195 s. The data revealed a single channel conductance of 65 ± 5.7 pS ($n = 3$) at negative potentials. 1 μM $LaCl_3$ was included in the bath and application solution.

rent of cells responding with I_{CRAC} (5 out of 10 cells) yielded an inward current of ∼−0.8 pA/pF at 300 s (data not shown). Representative *I*/*V* relationships for the H_2O_2 experiments are shown in Fig. 5F. These results suggest that activation of I_{CRAC} by H_2O_2 occurs mainly through a pathway involving IP_3 receptors, but that an IP_3 receptor-independent pathway can also lead to I_{CRAC}.

3.6. H_2O_2-induced activation of TPRM2 in Jurkat T lymphocytes

The activation of TRPM2 by H_2O_2 is well established [6–8], but with the activation of I_{CRAC} our results add a new aspect to the experimental use of H_2O_2. Jurkat T cells express both TRPM2 and I_{CRAC} endogenously [11,33]. However, the H_2O_2-induced Ca^{2+} influx observed after re-introduction of external Ca^{2+} could completely be blocked by 1 μM La^{3+} (Fig. 2B) and therefore is unlikely to represent Ca^{2+} influx through TRPM2 channels. Two questions therefore remain, why was TRPM2 mediated Ca^{2+} influx not apparent in Ca^{2+} imaging experiments, and if it is a matter of concentration, at what concentration does H_2O_2 activate TRPM2 in Jurkat T cells? We set out to measure H_2O_2-activated TRPM2 currents in patch-clamp experiments. Conditions used to investigate the activation of I_{CRAC} with intracellular Ca^{2+} clamped to 150 nM did not cause any TRPM2 activation in addition to I_{CRAC}, even when applying 500 μM H_2O_2 (data not shown). We therefore left intracellular Ca^{2+} unbuffered and assessed H_2O_2-induced single-channel activity that might reflect biophysical properties of TRPM2. This is possible in the whole-cell configuration because of the large single-channel conductance and characteristically long open times of TRPM2 channels [9,11,41]. Cells were kept in standard sodium solution with 1 mM $CaCl_2$ and 1 μM La^{3+}. Immediately after break-in, a recording with an 11 s long ramp protocol from −100 mV to 10 mV was started (Fig. 6) and 100 μM H_2O_2 was applied from the extracellular side. This produced only very few single channel openings in 3 out of 3 cells after 60 s. In two of the cells we observed activation of only 2 and 3 single channels and in another cell about 8 channels were active. Fig. 6 shows four ramp measurements from a representative recording with the activity of two single channels displaying a linear current with a reversal potential of 0 mV. We fitted the current traces of the first open channels in every cell with linear regression fits between −100 mV and 0 mV, yielding a mean single channel conductance of 65 ± 5.7 pS. This is very similar to the single channel conductances reported in Jurkat T cells when activating TRPM2 with ADPR, 67 pS, and cADPR, 69 pS [11]. These data, taken together with the measurements in intact cells (Fig. 2), indicate that H_2O_2 is a poor activator of TRPM2 in Jurkat T cells and the contribution of H_2O_2-activated TRPM2 channels to Ca^{2+} signals can therefore be regarded as negligible in this cell system.

4. Discussion

The current study provides evidence for H_2O_2 as a novel activator of the Ca^{2+}-selective CRAC current and thereby adds new knowledge to the involvement of H_2O_2 in regulating cellular calcium levels. Using calcium imaging and whole-cell patch-clamp

experiments we demonstrate that endogenous I_{CRAC} can be activated by extracellular application and intracellular perfusion of micromolar concentrations of H_2O_2 in Jurkat T cells, HEK293 cells, RBL-2H3 cells and DT40 B cells. This can be blocked by 1 μM $LaCl_3$. Heparin reduced the H_2O_2-activated I_{CRAC} in RBL-2H3 cells suggesting that IP_3 receptors play an important role in the Ca^{2+} release that leads to activation of I_{CRAC}. Furthermore electrophysiology experiments in DT40 WT and KO cells support the involvement of both IP_3-dependent and -independent mechanisms. Lastly, we confirm the activation of TRPM2 ion channels by H_2O_2 in Jurkat T cells, demonstrating that H_2O_2 within the same cell line is capable of activating both endogenous TRPM2 and CRAC channels.

Application of H_2O_2 has been reported to have different effects on ion channels, manifesting themselves as activation, potentiation or inhibition, but we are not aware of a report that would implicate activation of CRAC channels. There may be several explanations as to why other groups have not observed activation of I_{CRAC} by H_2O_2 in their experiments: First, the cell type in the given experiment may not produce significant I_{CRAC}. Second, endogenous I_{CRAC} is an exceedingly small current and requires optimized experimental conditions for electrophysiological detection, i.e. an enhanced Ca^{2+} gradient across the plasma membrane and buffering of cytosolic Ca^{2+} to prevent Ca^{2+}-induced inactivation. Third, due to its small amplitude, I_{CRAC} may not be detected in the presence of larger H_2O_2-activated currents.

In whole-cell patch-clamp experiments we investigated possible activation pathways of H_2O_2-induced I_{CRAC}. The lack of current response in HEK293 cells stably overexpressing CRACM1 speaks against a direct activation of CRAC channels by H_2O_2. Instead, it appears that Ca^{2+} release from intracellular stores may underlie this effect, since depletion of calcium stores is the main activation mechanism of I_{CRAC} and H_2O_2 has been reported to induce Ca^{2+} release via activation of IP_3 receptors in human platelets [36] and human endothelial cells [37]. This would also explain the observed reduction in H_2O_2-mediated I_{CRAC} amplitudes and delayed current activation kinetics when including heparin in the pipette solution. The involvement of IP_3R in H_2O_2-induced I_{CRAC} was further investigated in DT40 cells in which I_{CRAC}-like current development was observed in both WT and IP_3R KO cells when including H_2O_2 in the pipette solution. Based on these findings it is tempting to propose that H_2O_2 can also activate I_{CRAC} through IP_3-independent pathways.

A previous report suggested that H_2O_2 activates IP_3 receptors via oxidation of thiol groups, as a reduction in Ca^{2+} release was observed in endothelial cells when the reducing agent, dithiothreitol (DTT), was added to the bath solution [36]. The same study additionally ruled out that the H_2O_2-induced Ca^{2+} release occurred via an increased IP_3 production, although H_2O_2 may induce IP_3 production through activation of tyrosine kinases [42]. The latter effect may be further amplified through H_2O_2-mediated inhibition of protein tyrosine phosphatases [43]. Our results with heparin, which partially inhibits H_2O_2-induced activation I_{CRAC} (see Fig. 4), suggest that at least part of the H_2O_2 effect is mediated by IP_3 production, although we cannot rule out that heparin could also suppress a more direct activation of IP_3R.

In addition to the proposed involvement of IP_3R, H_2O_2 has also been reported to inhibit SERCA activity [36,44–46] and this could well be a contributing factor to Ca^{2+} store depletion leading to I_{CRAC}. The underlying mechanisms are not clear, but it has been suggested that this also occurs via oxidation of thiol groups, as one study observed a protective effect of DTT on SERCA [36]. Another report, however, found DTT to have equivocal effects on H_2O_2-induced inhibition of SERCA [45]. In the latter, a Fenton reaction ($Fe^{2+} + H_2O_2 \rightarrow OH^{\bullet} + OH^{-} + Fe^{3+}$) was used to generate hydroxyl radicals and thereby inducing oxidative stress in sarcoplasmic reticulum vesicles from rabbit skeletal muscle cells. Inhibition of SERCA could not be prevented by DTT when using Fe^{2+} in the Fenton reaction, but when replacing Fe^{2+} with Cu^{2+}, inhibition was completely abolished. Inhibition of SERCA by hydroxyl radicals has also been suggested to be due to a direct attack on the ATP-binding site [46]. In conclusion, both IP_3 receptors and SERCA may be responsible for H_2O_2-mediated store depletion and subsequent activation of I_{CRAC}.

Another possible contributor to store depletion by H_2O_2 could be increased membrane permeability through other pathways. The membrane of sarcoplasmic reticulum in pig coronary artery smooth muscle cells had a higher passive Ca^{2+} permeability when exposed to H_2O_2 than the plasma membrane [44], which would be in accordance with activation of I_{CRAC} by H_2O_2 while still maintaining cell integrity. Additional Ca^{2+}-release channels could be involved, e.g. RyR. This release channel can be activated by H_2O_2 [14] and induce ICRAC in DT40 B cells [47], but RBL-2H3 cells do not express RyR [48] and it is therefore not involved in activation of I_{CRAC} in these cells. This does not exclude RyR from contributing to H_2O_2-activated I_{CRAC} in other RyR expressing cell lines, e.g. DT40 B cells. It should be noted that the H_2O_2 concentration required for activation was in the millimolar range [14], which speaks against a significant contribution by RyR to the CRAC currents demonstrated in this study. It has recently been demonstrated that TRPM2 channels also function as lysosomal Ca^{2+}-release channels in (β-cells [49]. Our data do not exclude that TRPM2-mediated Ca^{2+} release can contribute to the activation of I_{CRAC}, but at least in Jurkat T cells, H_2O_2 is a rather weak activator of TRPM2 and not likely to contribute either to Ca^{2+} release or Ca^{2+} entry via TRPM2. Another possible source for Ca^{2+} release could be mitochondria, since several studies have reported mitochondrial Ca^{2+} release by H_2O_2 [36,37,50]. However, mitochondria are not considered as activators of I_{CRAC} and their role is to function as a Ca^{2+} buffer, thereby facilitating more extensive store depletion as well as reducing Ca^{2+}-dependent slow inactivation of I_{CRAC} [51]. Finally, it has been demonstrated that H_2O_2 releases Ca^{2+} from a thapsigargin-insensitive non-mitochondrial Ca^{2+} store in endothelial cells [37], raising the possibility that H_2O_2 could target an as yet unidentified CRAC store.

Lanthanides exert a blocking effect on several Ca^{2+}-conducting channels. Here we have used 1 μM $LaCl_3$, a potent blocker of I_{CRAC} with an estimated K_d of 58 nM [52], to confirm the H_2O_2-induced inward current as I_{CRAC}. It has been reported that exposing isolated sarcoplasmic reticulum vesicles to 15 μM La^{3+} also blocks IP_3 receptors [53], which could potentially lead to an indirect block of I_{CRAC}. This, however, does not appear to be the case in the present study, as we did not observe any major differences in the Ca^{2+}-release response of any of the cell lines when comparing H_2O_2 traces in the absence or presence of 1 μM $LaCl_3$. In addition, IP_3 receptors in our cells are unlikely to have been exposed directly to significant concentrations of La^{3+}, since La^{3+} does not easily cross membranes [54].

In this study we demonstrate the activation of I_{CRAC} both by external application of H_2O_2 as well as by internal perfusion. Since H_2O_2 appears to activate I_{CRAC} through store depletion, it likely interacts with components in intracellular stores and therefore requires H_2O_2 to cross the plasma membrane. This may explain differences in activation times and H_2O_2 concentrations required for activation of I_{CRAC} across different cell types, as they may differ in both membrane composition and expression of H_2O_2-transporting aquaporins. Additionally, differences in efficiency of cellular H_2O_2-eliminating mechanisms may influence the effective H_2O_2 concentration obtained for the activation of I_{CRAC} in a given cell. Interestingly, we found that activation of I_{CRAC} required a much lower H_2O_2 concentration than TRPM2 under optimized experimental conditions in Jurkat T cells where both mechanisms are present. This confirms that H_2O_2 may in principle serve as an

activator of TRPM2 currents but in Jurkat T cells it does so with much lower potency and efficacy than activating I_{CRAC}.

This study is the first to describe the activation of I_{CRAC} by H_2O_2, which adds new perspectives to the cross-talk between calcium homeostasis and ROS as well as to the use of H_2O_2 in experimental settings. This also means that the results of previous studies using H_2O_2 may have had Ca^{2+} contribution from I_{CRAC}, which could potentially affect both internal Ca^{2+} concentration as well as inward current amplitude in patch-clamp experiments. If I_{CRAC} activation is unwanted in experiments involving H_2O_2, addition of low concentrations of $LaCl_3$ may be a useful tool until selective I_{CRAC} inhibitors become available.

Given the broad spectrum of examples demonstrating cooperativity between H_2O_2 and Ca^{2+} it is highly probable that the findings of this study may be relevant in a number of processes, e.g. inflammation. Neutrophils produce substantial amount of H_2O_2 during the respiratory burst via NADPH oxidase and are highly dependent on intracellular Ca^{2+} as a trigger of processes such as adhesion, differentiation, chemotaxis, phagocytosis, oxidase activation and apoptosis [55]. Our findings provide a possible coupling between the H_2O_2 production and the cellular Ca^{2+} requirement. A similar scenario in which H_2O_2-activated I_{CRAC} could be relevant is the respiratory burst in mast cells in which ROS production, including H_2O_2, is accompanied by an increase in $[Ca^{2+}]_i$ via store-operated Ca^{2+} entry [56]. Furthermore it has been estimated that H_2O_2 during inflammation reaches concentrations of 10–100 μM in the microenvironment surrounding macrophages [57]. This falls within the concentrations used in this study for activation of I_{CRAC}. Finally, a recent study demonstrates that wound healing in zebra fish results in increased H_2O_2 concentration released by epithelial cells, extending as a concentration gradient 100–200 μm from the site of injury, presumably reaching concentrations of 0.5–50 μM gradually diminishing over 1–2 h [58]. The study further demonstrates that the released H_2O_2 functions as a chemotactic signal recruiting leukocytes to the damaged area. Although this contrasts the general concept that ROS produced during inflammation mainly originates from the respiratory burst of phagocytes, it provides an interesting scenario in which H_2O_2 can potentially function as a central mediator of Ca^{2+}-dependent processes in different immune cells.

Acknowledgements

We thank Nicole Schmitt for critical discussions and Stephanie Johne for excellent technical support. This work was supported in part by the Fulbright Scholarship (MGL, IIE grantee ID: 15089198), and NIHR01GM080555, R01GM063954 (RP).

Appendix A. Supplementary data

Supplementary data associated with this article can be found, in the online version, at doi:10.1016/j.ceca.2010.05.005.

References

[1] E.A. Veal, A.M. Day, B.A. Morgan, Hydrogen peroxide sensing and signaling, Mol. Cell 26 (2007) 1–14.
[2] Y. Yan, C.L. Wei, W.R. Zhang, H.P. Cheng, J. Liu, Cross-talk between calcium and reactive oxygen species signaling, Acta Pharmacol. Sin. 27 (2006) 821–826.
[3] G.P. Bienert, A.L. Moller, K.A. Kristiansen, A. Schulz, I.M. Moller, J.K. Schjoerring, T.P. Jahn, Specific aquaporins facilitate the diffusion of hydrogen peroxide across membranes, J. Biol. Chem. 282 (2007) 1183–1192.
[4] L.C. Hool, B. Corry, Redox control of calcium channels: from mechanisms to therapeutic opportunities, Antioxid. Redox Signal. 9 (2007) 409–435.
[5] J.I. Kourie, Interaction of reactive oxygen species with ion transport mechanisms, Am. J. Physiol. 275 (1998) C1–24.
[6] Y. Hara, M. Wakamori, M. Ishii, E. Maeno, M. Nishida, T. Yoshida, H. Yamada, S. Shimizu, E. Mori, J. Kudoh, N. Shimizu, H. Kurose, Y. Okada, K. Imoto, Y. Mori, LTRPC2 Ca^{2+}-permeable channel activated by changes in redox status confers susceptibility to cell death, Mol. Cell 9 (2002) 163–173.
[7] M. Kolisek, A. Beck, A. Fleig, R. Penner, Cyclic ADP-ribose and hydrogen peroxide synergize with ADP-ribose in the activation of TRPM2 channels, Mol. Cell 18 (2005) 61–69.
[8] E. Wehage, J. Eisfeld, I. Heiner, E. Jungling, C. Zitt, A. Luckhoff, Activation of the cation channel long transient receptor potential channel 2 (LTRPC2) by hydrogen peroxide. A splice variant reveals a mode of activation independent of ADP-ribose, J. Biol. Chem. 277 (2002) 23150–23156.
[9] A.L. Perraud, A. Fleig, C.A. Dunn, L.A. Bagley, P. Launay, C. Schmitz, A.J. Stokes, Q. Zhu, M.J. Bessman, R. Penner, J.P. Kinet, A.M. Scharenberg, ADP-ribose gating of the calcium-permeable LTRPC2 channel revealed by Nudix motif homology, Nature 411 (2001) 595–599.
[10] Y. Sano, K. Inamura, A. Miyake, S. Mochizuki, H. Yokoi, H. Matsushime, K. Furuichi, Immunocyte Ca^{2+} influx system mediated by LTRPC2, Science 293 (2001) 1327–1330.
[11] A. Beck, M. Kolisek, L.A. Bagley, A. Fleig, R. Penner, Nicotinic acid adenine dinucleotide phosphate and cyclic ADP-ribose regulate TRPM2 channels in T lymphocytes, Faseb J. 20 (2006) 962–964.
[12] I. Lange, R. Penner, A. Fleig, A. Beck, Synergistic regulation of endogenous TRPM2 channels by adenine dinucleotides in primary human neutrophils, Cell Calcium 44 (2008) 604–615.
[13] A.L. Perraud, C.L. Takanishi, B. Shen, S. Kang, M.K. Smith, C. Schmitz, H.M. Knowles, D. Ferraris, W. Li, J. Zhang, B.L. Stoddard, A.M. Scharenberg, Accumulation of free ADP-ribose from mitochondria mediates oxidative stress-induced gating of TRPM2 cation channels, J. Biol. Chem. 280 (2005) 6138–6148.
[14] A. Boraso, A.J. Williams, Modification of the gating of the cardiac sarcoplasmic reticulum Ca(2+)-release channel by H_2O_2 and dithiothreitol, Am. J. Physiol. 267 (1994) H1010–H1016.
[15] M. Aarts, K. Iihara, W.L. Wei, Z.G. Xiong, M. Arundine, W. Cerwinski, J.F. MacDonald, M. Tymianski, A key role for TRPM7 channels in anoxic neuronal death, Cell 115 (2003) 863–877.
[16] F. Mendez, R. Penner, Near-visible ultraviolet light induces a novel ubiquitous calcium-permeable cation current in mammalian cell lines, J. Physiol. 507 (Pt 2) (1998) 365–377.
[17] M. Hoth, R. Penner, Depletion of intracellular calcium stores activates a calcium current in mast cells, Nature 355 (1992) 353–356.
[18] J. Liou, M.L. Kim, W.D. Heo, J.T. Jones, J.W. Myers, J.E. Ferrell Jr., T. Meyer, STIM is a Ca^{2+} sensor essential for Ca^{2+}-store-depletion-triggered Ca^{2+} influx, Curr. Biol. 15 (2005) 1235–1241.
[19] J. Roos, P.J. DiGregorio, A.V. Yeromin, K. Ohlsen, M. Lioudyno, S. Zhang, O. Safrina, J.A. Kozak, S.L. Wagner, M.D. Cahalan, G. Velicelebi, K.A. Stauderman, STIM1, an essential and conserved component of store-operated Ca^{2+} channel function, J. Cell Biol. 169 (2005) 435–445.
[20] S. Feske, Y. Gwack, M. Prakriya, S. Srikanth, S.H. Puppel, B. Tanasa, P.G. Hogan, R.S. Lewis, M. Daly, A. Rao, A mutation in Orai1 causes immune deficiency by abrogating CRAC channel function, Nature 441 (2006) 179–185.
[21] M. Vig, C. Peinelt, A. Beck, D.L. Koomoa, D. Rabah, M. Koblan-Huberson, S. Kraft, H. Turner, A. Fleig, R. Penner, J.P. Kinet, CRACM1 is a plasma membrane protein essential for store-operated Ca^{2+} entry, Science 312 (2006) 1220–1223.
[22] S.L. Zhang, A.V. Yeromin, X.H. Zhang, Y. Yu, O. Safrina, A. Penna, J. Roos, K.A. Stauderman, M.D. Cahalan, Genome-wide RNAi screen of Ca(2+) influx identifies genes that regulate Ca(2+) release-activated Ca(2+) channel activity, Proc. Natl. Acad. Sci. U.S.A. 103 (2006) 9357–9362.
[23] S. Parvez, A. Beck, C. Peinelt, J. Soboloff, A. Lis, M. Monteilh-Zoller, D.L. Gill, A. Fleig, R. Penner, STIM2 protein mediates distinct store-dependent and store-independent modes of CRAC channel activation, Faseb J. 22 (2008) 752–761.
[24] C. Peinelt, M. Vig, D.L. Koomoa, A. Beck, M.J. Nadler, M. Koblan-Huberson, A. Lis, A. Fleig, R. Penner, J.P. Kinet, Amplification of CRAC current by STIM1 and CRACM1 (Orai1), Nat. Cell Biol. 8 (2006) 771–773.
[25] J. Soboloff, M.A. Spassova, T. Hewavitharana, L.P. He, W. Xu, L.S. Johnstone, M.A. Dziadek, D.L. Gill, STIM2 is an inhibitor of STIM1-mediated store-operated Ca^{2+} entry, Curr. Biol. 16 (2006) 1465–1470.
[26] J. Eisfeld, A. Luckhoff, Trpm2, Handb. Exp. Pharmacol. (2007) 237–252.
[27] K. Togashi, H. Inada, M. Tominaga, Inhibition of the transient receptor potential cation channel TRPM2 by 2-aminoethoxydiphenyl borate (2-APB), Br. J. Pharmacol. 153 (2008) 1324–1330.
[28] J.W. Daly, J. Lueders, W.L. Padgett, Y. Shin, F. Gusovsky, Maitotoxin-elicited calcium influx in cultured cells. Effect of calcium-channel blockers, Biochem. Pharmacol. 50 (1995) 1187–1197.
[29] M. Prakriya, R.S. Lewis, Potentiation and inhibition of Ca(2+) release-activated Ca(2+) channels by 2-aminoethyldiphenyl borate (2-APB) occurs independently of IP(3) receptors, J. Physiol. 536 (2001) 3–19.
[30] S. Schumann, R. Greger, J. Leipziger, Flufenamate and Gd3+ inhibit stimulated Ca^{2+} influx in the epithelial cell line CFPAC-1, Pflugers Arch. 428 (1994) 583–589.
[31] M. Hoth, R. Penner, Calcium release-activated calcium current in rat mast cells, J. Physiol. 465 (1993) 359–386.
[32] R. Kraft, C. Grimm, K. Grosse, A. Hoffmann, S. Sauerbruch, H. Kettenmann, G. Schultz, C. Harteneck, Hydrogen peroxide and ADP-ribose induce TRPM2-mediated calcium influx and cation currents in microglia, Am. J. Physiol. Cell Physiol. 286 (2004) C129–C137.
[33] A. Zweifach, R.S. Lewis, Mitogen-regulated Ca^{2+} current of T lymphocytes is activated by depletion of intracellular Ca^{2+} stores, Proc. Natl. Acad. Sci. U.S.A. 90 (1993) 6295–6299.

[34] C. Fasolato, M. Hoth, R. Penner, A GTP-dependent step in the activation mechanism of capacitative calcium influx, J. Biol. Chem. 268 (1993) 20737–20740.
[35] B. Moreau, S. Straube, R.J. Fisher, J.W. Putney Jr., A.B. Parekh, Ca^{2+}-calmodulin-dependent facilitation and Ca^{2+} inactivation of Ca^{2+} release-activated Ca^{2+} channels, J. Biol. Chem. 280 (2005) 8776–8783.
[36] P.C. Redondo, G.M. Salido, J.A. Rosado, J.A. Pariente, Effect of hydrogen peroxide on Ca^{2+} mobilisation in human platelets through sulphydryl oxidation dependent and independent mechanisms, Biochem. Pharmacol. 67 (2004) 491–502.
[37] Y. Zheng, X. Shen, H_2O_2 directly activates inositol 1,4,5-trisphosphate receptors in endothelial cells, Redox Rep. 10 (2005) 29–36.
[38] T.K. Ghosh, P.S. Eis, J.M. Mullaney, C.L. Ebert, D.L. Gill, Competitive, reversible, and potent antagonism of inositol 1,4,5-trisphosphate-activated calcium release by heparin, J. Biol. Chem. 263 (1988) 11075–11079.
[39] H. Sugawara, M. Kurosaki, M. Takata, T. Kurosaki, Genetic evidence for involvement of type 1, type 2 and type 3 inositol 1,4,5-trisphosphate receptors in signal transduction through the B-cell antigen receptor, EMBO J. 16 (1997) 3078–3088.
[40] C. Peinelt, A. Beck, M.K. Monteilh-Zoller, R. Penner, A. Fleig, IP(3) receptor subtype-dependent activation of store-operated calcium entry through I(CRAC), Cell Calcium 45 (2009) 326–330.
[41] P.S. Herson, K.A. Dulock, M.L. Ashford, Characterization of a nicotinamide-adenine dinucleotide-dependent cation channel in the CRI-G1 rat insulinoma cell line, J. Physiol. 505 (Pt 1) (1997) 65–76.
[42] S. Qin, T. Inazu, M. Takata, T. Kurosaki, Y. Homma, H. Yamamura, Cooperation of tyrosine kinases p72syk and p53/56lyn regulates calcium mobilization in chicken B cell oxidant stress signaling, Eur. J. Biochem. 236 (1996) 443–449.
[43] T.C. Meng, T. Fukada, N.K. Tonks, Reversible oxidation and inactivation of protein tyrosine phosphatases in vivo, Mol. Cell 9 (2002) 387–399.
[44] A.K. Grover, S.E. Samson, V.P. Fomin, Peroxide inactivates calcium pumps in pig coronary artery, Am. J. Physiol. 263 (1992) H537–H543.
[45] V.H. Moreau, R.F. Castilho, S.T. Ferreira, P.C. Carvalho-Alves, Oxidative damage to sarcoplasmic reticulum Ca^{2+}-ATPase AT submicromolar iron concentrations: evidence for metal-catalyzed oxidation, Free Radic. Biol. Med. 25 (1998) 554–560.
[46] K.Y. Xu, J.L. Zweier, L.C. Becker, Hydroxyl radical inhibits sarcoplasmic reticulum Ca(2+)-ATPase function by direct attack on the ATP binding site, Circ Res 80 (1997) 76–81.
[47] K. Kiselyov, D.M. Shin, N. Shcheynikov, T. Kurosaki, S. Muallem, Regulation of Ca^{2+}-release-activated Ca^{2+} current (I_{CRAC}) by ryanodine receptors in inositol 1,4,5-trisphosphate-receptor-deficient DT40 cells, Biochem. J. 360 (2001) 17–22.
[48] D.L. Bennett, T.R. Cheek, M.J. Berridge, H. De Smedt, J.B. Parys, L. Missiaen, M.D. Bootman, Expression and function of ryanodine receptors in nonexcitable cells, J. Biol. Chem. 271 (1996) 6356–6362.
[49] I. Lange, S. Yamamoto, S. Partida-Sanchez, Y. Mori, A. Fleig, R. Penner, TRPM2 functions as a lysosomal Ca^{2+}-release channel in beta cells, Sci. Signal 2 (2009) ra23.
[50] J.A. Pariente, C. Camello, P.J. Camello, G.M. Salido, Release of calcium from mitochondrial and nonmitochondrial intracellular stores in mouse pancreatic acinar cells by hydrogen peroxide, J. Membr. Biol. 179 (2001) 27–35.
[51] M.D. Glitsch, D. Bakowski, A.B. Parekh, Store-operated Ca^{2+} entry depends on mitochondrial Ca^{2+} uptake, EMBO J. 21 (2002) 6744–6754.
[52] P.E. Ross, M.D. Cahalan, Ca^{2+} influx pathways mediated by swelling or stores depletion in mouse thymocytes, J. Gen. Physiol. 106 (1995) 415–444.
[53] M. Magocsi, A. Enyedi, B. Sarkadi, G. Gardos, Effects of phosphoinositides on calcium movements in human platelet membrane vesicles, Biochim. Biophys. Acta 944 (1988) 202–212.
[54] C.Y. Kwan, J.W. Putney Jr., Uptake and intracellular sequestration of divalent cations in resting and methacholine-stimulated mouse lacrimal acinar cells. Dissociation by Sr^{2+} and Ba^{2+} of agonist-stimulated divalent cation entry from the refilling of the agonist-sensitive intracellular pool, J. Biol. Chem. 265 (1990) 678–684.
[55] W. Tian, S. Dewitt, I. Laffafian, M.B. Hallett, Ca(2+), calpain and 3-phosphorylated phosphatidyl inositides; decision-making signals in neutrophils as potential targets for therapeutics, J. Pharm. Pharmacol. 56 (2004) 565–571.
[56] Y. Suzuki, T. Yoshimaru, T. Matsui, T. Inoue, O. Niide, S. Nunomura, C. Ra, Fc epsilon RI signaling of mast cells activates intracellular production of hydrogen peroxide: role in the regulation of calcium signals, J. Immunol. 171 (2003) 6119–6127.
[57] W. Droge, Free radicals in the physiological control of cell function, Physiol. Rev. 82 (2002) 47–95.
[58] P. Niethammer, C. Grabher, A.T. Look, T.J. Mitchison, A tissue-scale gradient of hydrogen peroxide mediates rapid wound detection in zebrafish, Nature 459 (2009) 996–999.